

Formulation of Resonance Frequency for Multi-Band Circular Microstrip Antennas

A. A. Deshmukh^{1*}, K. P. Ray², T. Sonawdekar¹, S. Varawalla¹ and R. Kataria¹

1. DJSCOE, Vile – Parle (W), Mumbai – 400 056, India

2. SAMEER, I.I.T. Campus, Powai, Mumbai – 400 076, India

Tel: 91 22 2610 7010, Fax: 91 22 2619 4988, Email: - amitdeshmukh76@yahoo.com, kpray@rediffmail.com

Abstract- One of the many techniques for realizing a multi-band microstrip antenna is by cutting a slot inside the patch. The slot whose length is either quarter wave or half wave in length, when cut inside the patch introduces a mode near the patch frequency and realizes dual frequency response. However this simpler approximation of slot length against the frequency does not give closer results over the wide range of slot dimensions. In this paper, by studying the surface current distributions for slotted circular microstrip antennas, a formulation of resonant length for slot mode is proposed. The slot frequency calculated by using these proposed equations agrees well with the simulated results with an error of less than 5%.

Index Terms- circular microstrip antenna, dual band microstrip antenna, U-slot, pair of rectangular slots

I. INTRODUCTION

The dual band microstrip antenna (MSA) is realized by cutting the slots of different shapes like, U-slot, V-slot, pair of rectangular slots and step slots, etc [1 – 10]. The slot when its length is either quarter wavelength when cut on the edges of the MSA or half wavelength, when cut inside the MSA, introduces a mode near the patch mode and realizes dual band response. However, towards the shorted end of the slot, surface currents encircle over a finite length. This adds to the additional length and therefore by adding a correction length, a better approximation of slot length against the frequency is obtained [11]. The Broadband MSAs using these slots are also realized when the coupling between the slot and patch modes is controlled, such that the loop formed in the input impedance locus lies completely inside the VSWR = 2 circle [1, 12 – 15]. Using the variations of rectangular slots and

U-slots, a broadband circular MSA (CMSA) are realized [16]. However, in these dual band as well as broadband MSAs, these simpler approximations of slot length against the frequency does not give closer results for wide range of slot dimensions and their positions. Therefore, in-depth analysis of slotted CMSAs for mode variation over a wide frequency range is needed to formulate the resonant length for the slot mode.

In this paper, the surface current distributions generated using IE3D software [17] for dual band pair of rectangular slot and U-slot cut CMSA for various slot lengths and their positions inside the patch are studied. It was observed that, the slot does not introduce any mode but reduces the second order resonance frequency of CMSA and along with fundamental mode gives the dual band response. The formulations of resonant length for the patch as well as slot mode (modified higher order mode) is proposed. The resonance frequencies obtained using these formulations agrees well with the simulated results obtained using IE3D software over the entire slot length range. These formulations are first proposed on glass epoxy substrate ($\epsilon_r = 4.3$, $h = 0.16$ cm, $\tan \delta = 0.02$). Further they are validated on RT-duroid substrate ($\epsilon_r = 2.33$, $h = 0.16$ cm, $\tan \delta = 0.001$).

II. DUAL BAND CMSAs

The CMSA with radius (r) = 4.5 cm, on glass epoxy substrate has the TM_{11} mode resonance frequency of 950 MHz. This CMSA has TM_{21} and TM_{20} mode resonance frequencies of 1562 and 1963 MHz, respectively. The surface current distributions for first two modes are shown in Fig. 1(a, b). To realize a dual band response, the slots are cut inside this CMSA. A dual band

CMSA with pair of rectangular slot cut on its edge is shown in Fig. 2(a). The current distributions at dual frequencies for different slot length (l_s) and its position (Y) from feed point axis were studied and for $l_s = 2.0$ cm, $w = 0.4$ cm and $Y = 1.0$ cm, they are shown in Fig. 2(b, c).

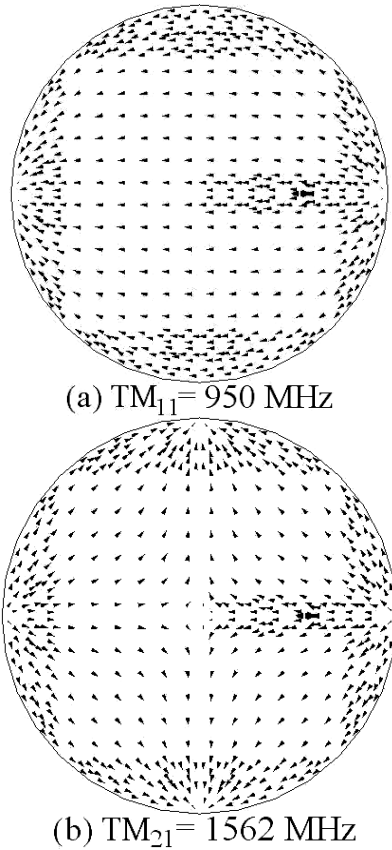


Fig. 1 (a, b) Surface current distributions for CMSA

As seen from the current distributions, the slot reduces TM_{21} frequency from 1562 MHz to 1381 MHz and the second frequency (f_2) is governed by the TM_{21} mode. At first frequency ($f_1 = 945$ MHz), TM_{11} mode is dominant as half wavelength variation along half of the perimeter is observed. This current distribution is also perturbed by the dual slots and the f_1 is slightly reduced. Thus, the slots do not introduce any mode but reduces the TM_{21} frequency and along with TM_{11} mode realizes dual band response. Similarly a dual band pair of slots cut (slots cut inside the patch) or U-slot cut CMSA and current distributions at respective dual frequencies are shown in Figs. 3 and 4, respectively.

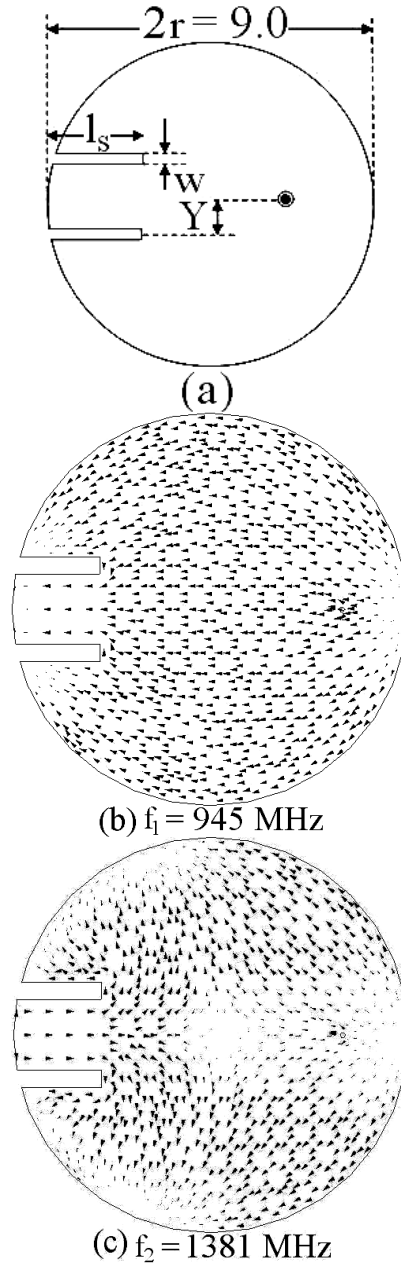


Fig. 2 (a) Pair of rectangular slots cut CMSA and its (b, c) surface current distributions at dual frequencies

As seen from the current distributions, the pair of slots and the U-slot reduces the TM_{11} and TM_{21} mode resonance frequencies and the f_1 and f_2 are governed by the modified TM_{11} and TM_{21} mode, respectively. The radiation pattern for CMSA at TM_{11} and TM_{21} mode is in the broadside and conical directions, respectively. In these dual band CMSAs, the radiation pattern at f_1 is in the broadside direction. However, since the slots affects the current distribution on the patch, with

the increasing slot length, the radiation pattern at f_2 becomes in the broadside direction. In the following sections, by studying the surface current distributions, the formulations of the resonant length at the dual frequencies are proposed.

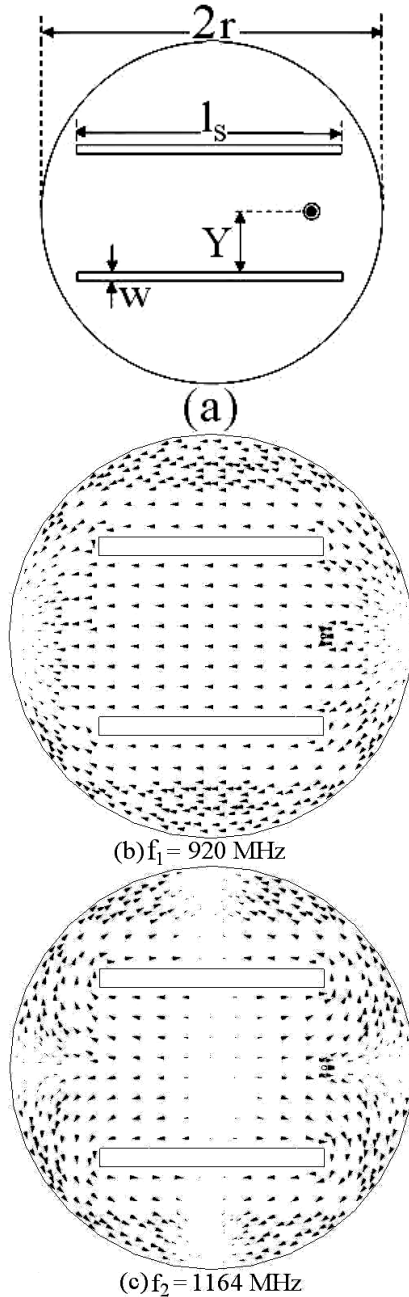


Fig. 3 (a) Pair of rectangular slots cut CMSA and its (b, c) surface current distributions at dual frequencies

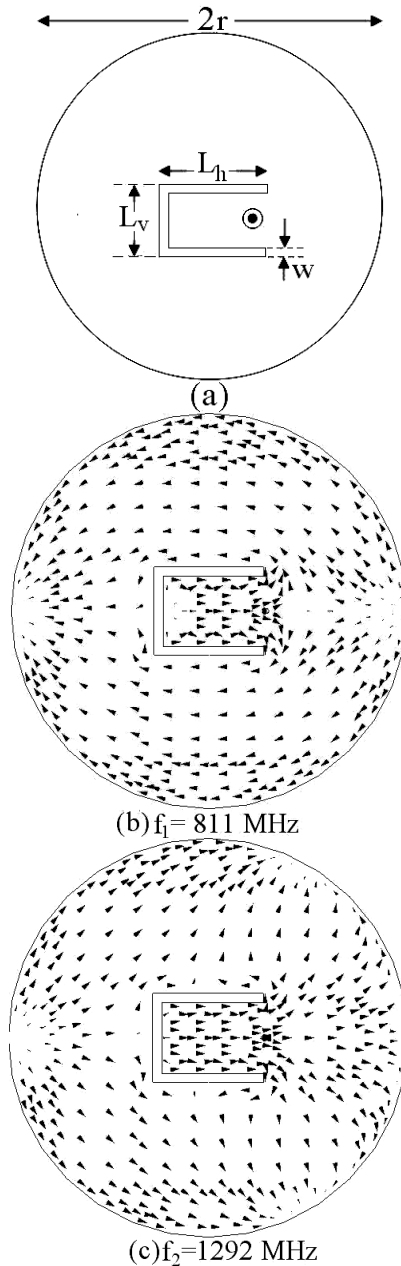


Fig. 4 (a) U-slot cut CMSA and its (b, c) surface current distributions at dual frequencies

II. FORMULATION OF RESONANT LENGTH FOR DUAL BAND CMSAs

The resonant frequency for CMSA (f_r) is calculated by using equation (1).

$$f_r = c K_{nm} / 2\pi r_e (\epsilon_r)^{1/2} \tag{1}$$

Where,

r_e = effective CMSA radius
 $K_{nm} = 1.84118$ (TM₁₁), 3.05424 (TM₂₁)

For dual band CMSA as shown in Fig. 2(a), for smaller values of l_s ($l_s < r$), the decrease in f_1 is smaller whereas for $l_s > r$, decrease in f_1 is larger. The f_2 first decreases with increase in l_s , whereas for $l_s > r$, it nearly remains constant. This different variation in dual frequencies is due to the difference in the current distributions at TM₁₁ and TM₂₁ modes. Therefore for different values of Y , f_2 is formulated for $l_s = 1$ to 5 cm whereas f_1 is formulated for $l_s = 2$ to 8 cm. As observed from current distribution, the slot increases surface current length and effectively modifies r_e . By changing r_e with respect to l_s , the resonant length (frequency) formulation is obtained as given in equations (2) – (5).

At f_1 ,

$$r_{e1} = r_e + 2Al_s \sin(\pi Y/r) \quad (2)$$

$$A = (l_s / 4r) \sin(\pi l_s / 4r) \quad (3)$$

$$f_1 = c K_{nm} / 2\pi r_{e1} (\epsilon_r)^{1/2} \quad (4)$$

$$E = 100 ((f_{ie3d} - f_1) / f_{ie3d}) \quad (5)$$

Where,

- r_{e1} = effective patch radius due to the slot
- f_1 = calculated first frequency
- f_{ie3d} = simulated frequency
- E = % error between the two frequencies

The factor ‘2’ in equation (2) is to account for circulation of currents around slot length. Also the perturbation in current length depends upon l_s . This is modeled by using a weighting function (A). The equation for A is derived based on the given mode and variation in frequency with respect to l_s . For a given l_s , the frequency reduces with increase in Y , since the slots are placed towards the maximum current location in both the modes. To account for this variation, a sinusoidal function is used in equation (2). The frequency is calculated using equation (4) and the % error (E) between the calculated and simulated values with respect to simulated value is calculated using equation (5) and they are plotted

in Fig. 5(a – c). The formulation in resonant length at f_2 is obtained by using equations (6) and (7).

At f_2 ,

$$r_{e1} = r_e + 2Al_s \sin(\pi Y/r) \quad (6)$$

$$A = (l_s / 2r) \sin(\pi l_s / 2r) \quad (7)$$

$$f_2 = c K_{nm} / 2\pi r_{e1} (\epsilon_r)^{1/2} \quad (8)$$

$$E = 100 ((f_{ie3d} - f_2) / f_{ie3d}) \quad (9)$$

Where,

f_2 = calculated second frequency

Here, the equation for A is derived based on TM₂₁ mode and variation in its frequency with respect to l_s . The f_2 and E is calculated by using equations (8) and (9) and they are plotted in Fig. 6(a – c). For the dual band CMSA with pair of slots cut inside the patch (Fig. 3(a)), the reduction in f_1 is negligible, as w is smaller. However slot modifies the current length at f_2 and the formulation in the resonant length is obtained by using equations (10) and (11).

At f_2 ,

$$r_{e1} = r_e + 2Al_s \sin(\pi Y/r) \quad (10)$$

$$A = (l_s / 2.2r) \sin(\pi l_s / 5.6r) \quad (11)$$

Since the perturbation in current length increases with l_s , similar to the above dual band CMSA formulation, a weighting function is used whose value increases with l_s . The value of A is calculated depending upon the variation in frequency against l_s for TM₂₁ mode. To account for variation in frequency with respect to Y , the sinusoidal term is included in equation (10). The f_2 and E are calculated by using equation (8) and (9), respectively. For $Y = 1$ to 3 cm, the frequencies calculated using proposed formulation and using IE3D and the E plots, are shown in Fig. 7(a – c).

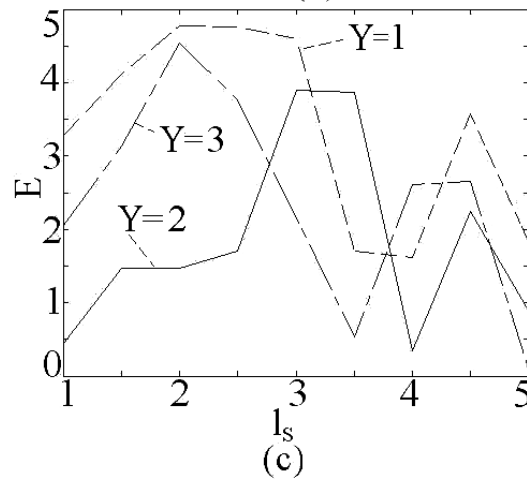
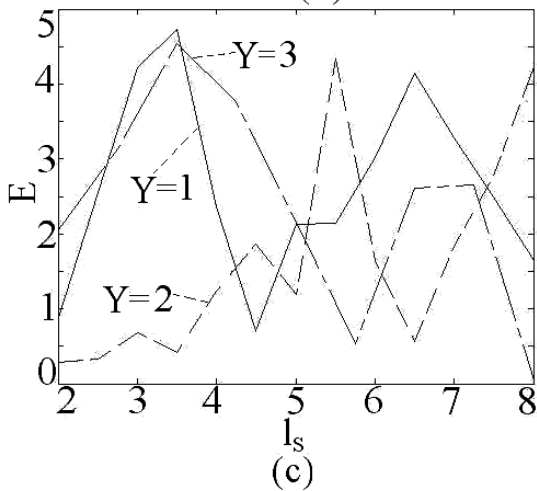
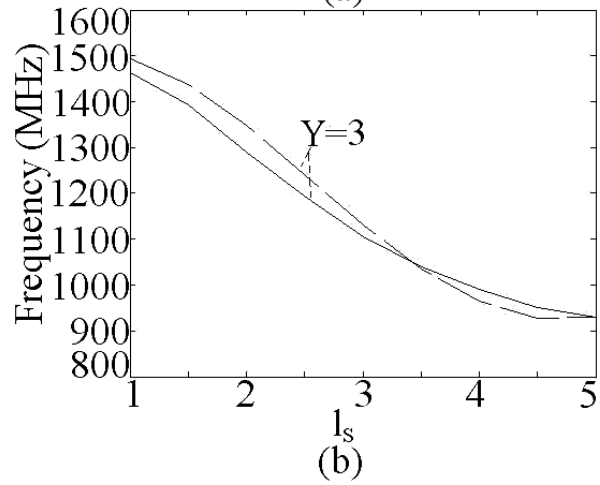
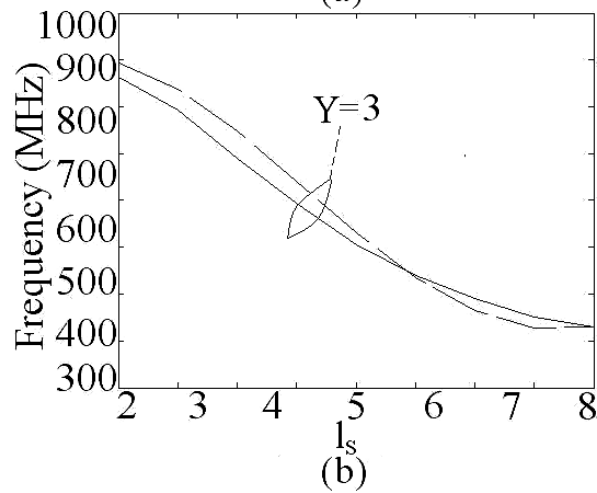
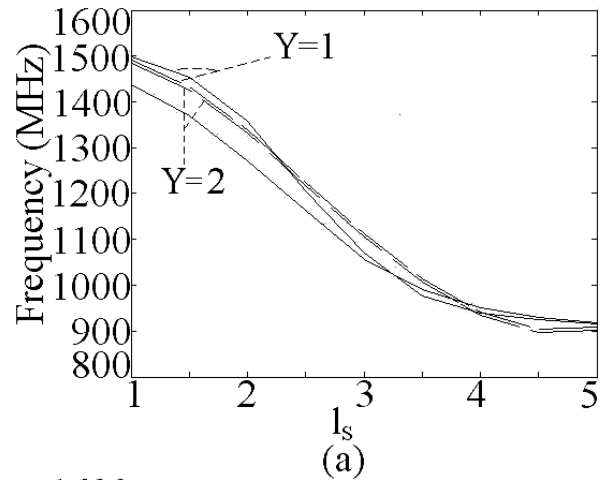
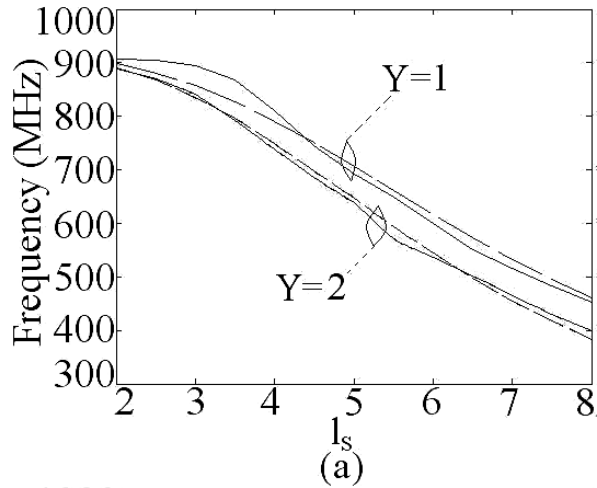


Fig. 5 (a, b) Resonance frequency and (c) E plots at f_1 for pair of rectangular slots cut CMSA, (—) IE3D, (---) Proposed method

Fig. 6 (a, b) Resonance frequency and (c) E plots at f_2 for pair of rectangular slots cut CMSA, (—) IE3D, (---) Proposed method

As seen from the current distributions for U-slot cut CMSA, the slot reduces TM_{11} and TM_{21} mode resonance frequencies and realizes dual band response. Here, the vertical U-slot length (L_v) is

orthogonal to surface currents at TM_{11} mode, and it largely affects f_1 . Whereas the horizontal slot length (L_h) is orthogonal to surface currents at TM_{21} mode and it affects f_2 .

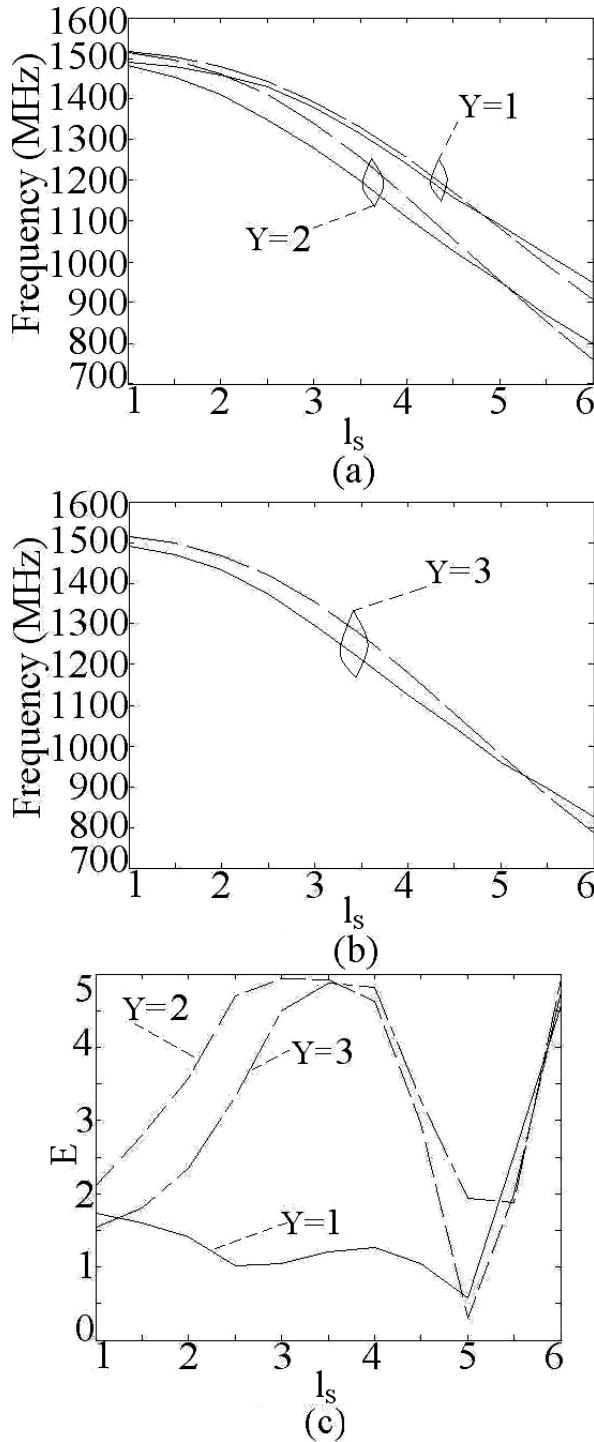


Fig. 7 (a, b) Resonance frequency and (c) E plots at f_2 for pair of rectangular slots cut inside CMSA, (—) IE3D, (---) Proposed method

The r_e is modified with respect to L_h and L_v to realize formulation of resonant length at f_1 as given in equations (12) and (13).

$$r_{e1} = r_e + BL_v + AL_h \quad (12)$$

$$A = (L_h/C) (\sin(\pi L_h/2.2r))^{1/2} \quad (13)$$

The values of A, B and C used in above equations are selected depending upon the perturbation in surface current length with respect to slot dimensions. For smaller U-slot dimensions ($L_v \leq r/4$) the perturbation in the surface currents is minimum. In those cases, a better prediction in the resonant length is obtained by using $B = 0.15$ and $C = 4.8$. With increase in L_v , the perturbation in surface current increases and for $L_v \geq r/4$, using $B = 0.35$ and $C = 3$, a closer agreement between the calculated and simulated frequencies is obtained. The f_1 and E are calculated using equations (4) and (5). For $L_v = 1.0$ to 5.0 cm, and $L_h = 2$ to 6 cm, the calculated and simulated frequencies and E are shown in Figs. 8(a – c) and 9(a, b). At f_2 , the formulation in resonant length is obtained by using equations (14) and (15).

$$r_{e1} = r_e + 1.5AL_h \sin(\pi L_v/2r) \quad (14)$$

$$A = (L_h/C) (\sin(\pi L_h/Dr))^{1/2} \quad (15)$$

Similar to the above, the perturbation in surface currents depends upon L_v . For $L_v \leq r/4$, using C and $D = 2.5$, a closer prediction in resonant length is obtained and for $L_v \geq r/4$, using $C = 1.8$ and $D = 1.5$, a closer prediction between the two frequencies is obtained. The frequencies and E plots at f_2 are shown in Figs. 9(c, d) and Fig. 10.

These formulations are also validated on RT-duroid substrate. The patch radius to have TM_{11} frequency equal to 950 MHz on RT-duroid substrate is 6.0 cm. For CMSA with pair of slots cut inside the patch, the frequencies and E plots calculated using equations (10), (11), (8) and (9) are shown in Fig. 11(a – c).

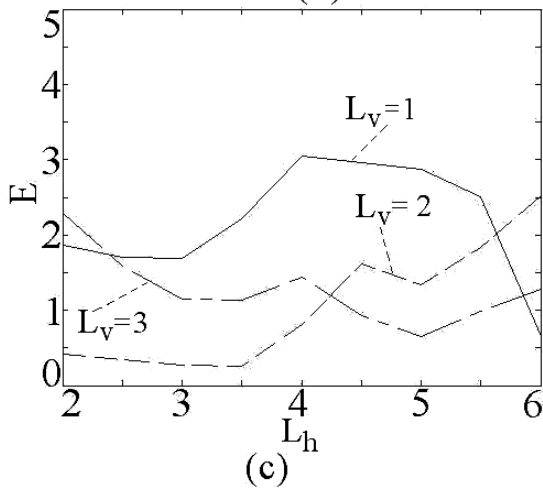
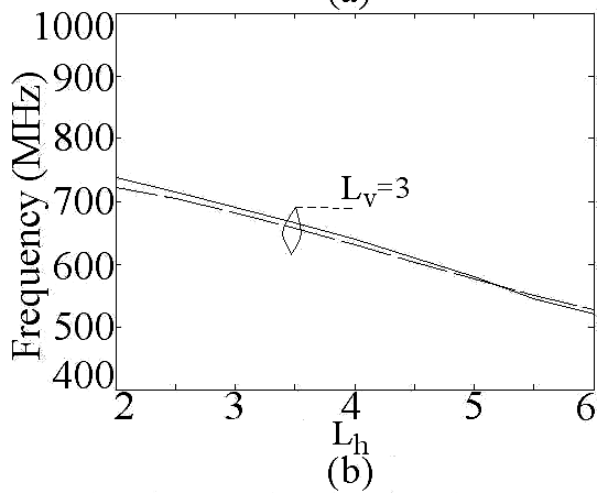
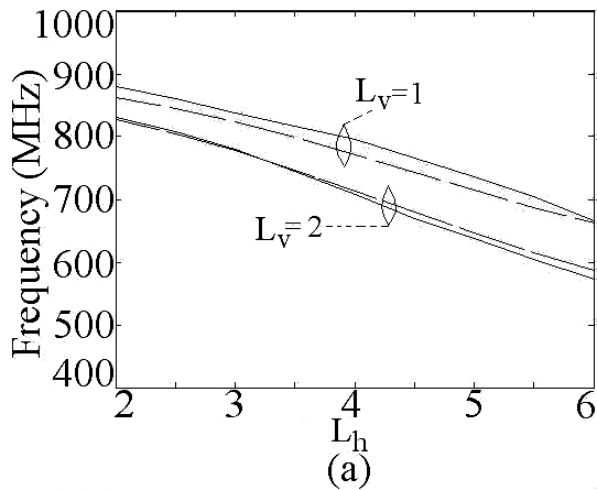


Fig. 8 (a, b) Resonance frequency and (c) E plots at f_1 for U-slot cut CMSA, (—) IE3D, (---) Proposed method

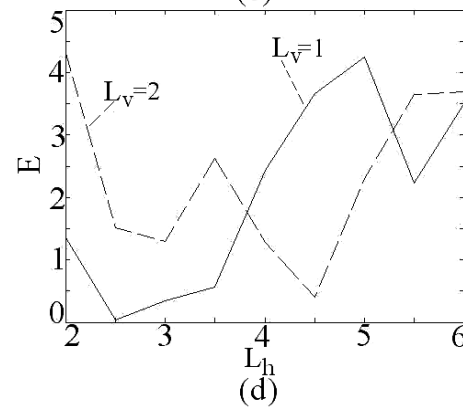
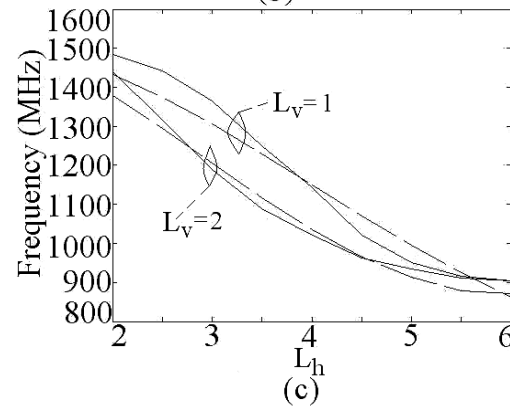
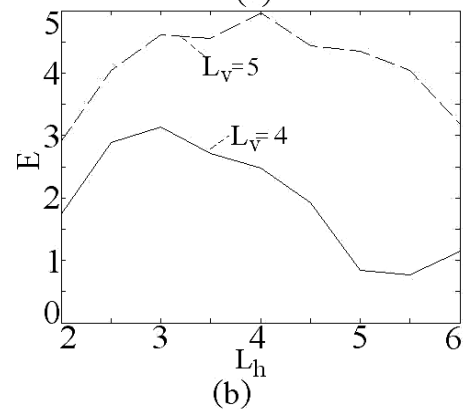
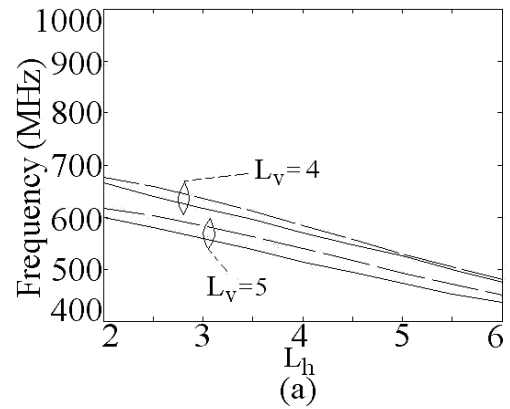


Fig. 9 Resonance frequency and E plots at (a - b) f_1 and (c - d) f_2 for U-slot cut CMSA, (—) IE3D, (---) Proposed method

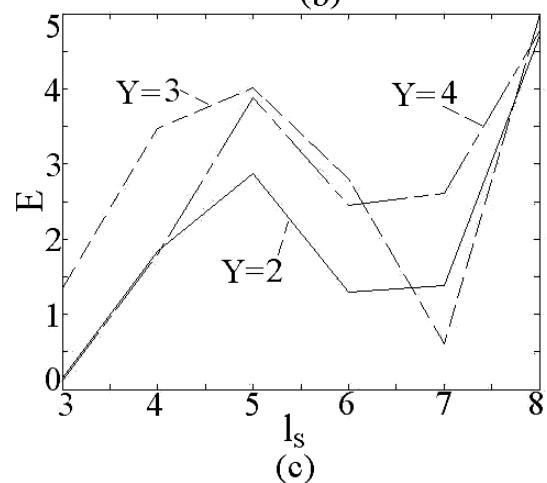
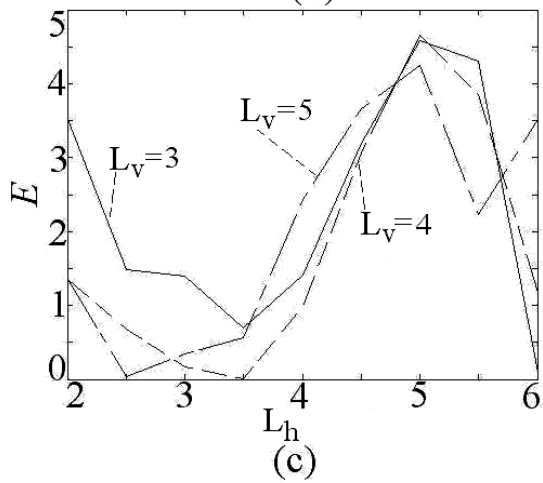
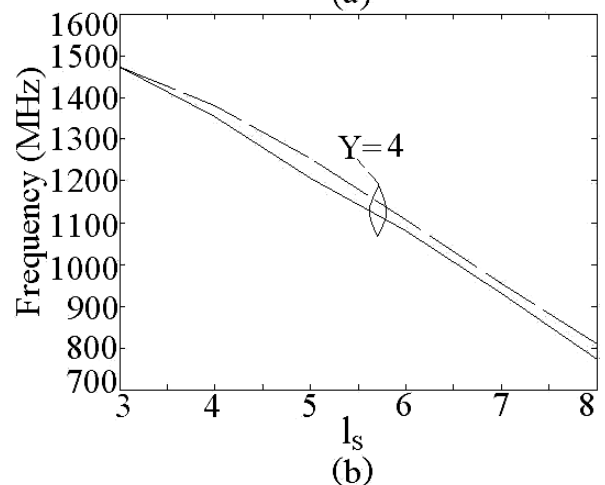
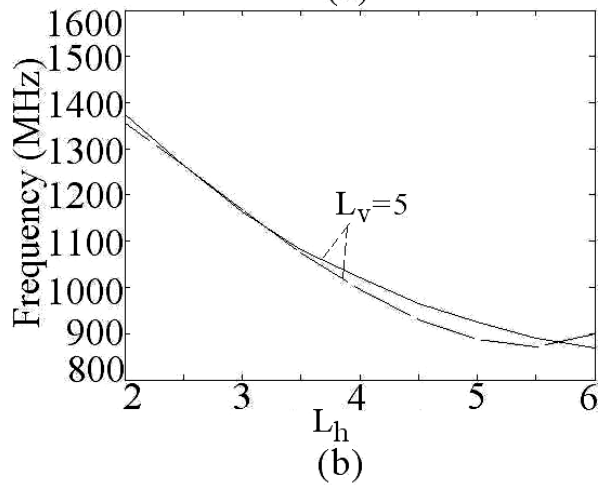
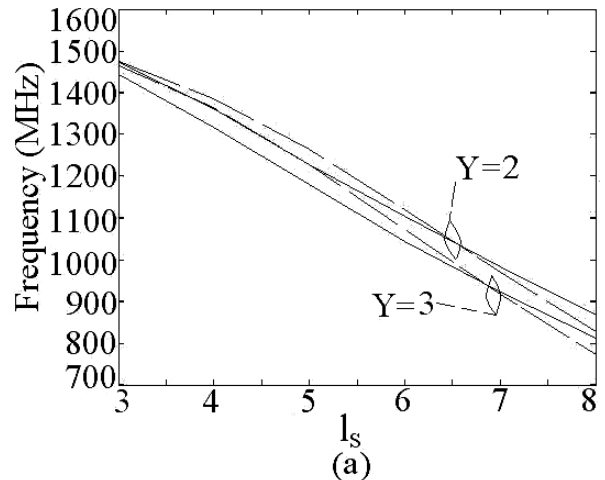
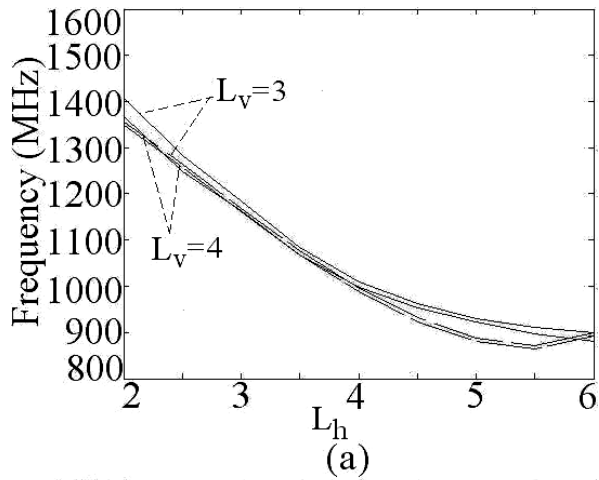


Fig. 10 (a, b) Resonance frequency and (c) E plot at f_2 for U-slot cut CMSA, (—) IE3D, (---) Proposed method

Fig. 11 (a, b) Resonance frequency and (c) E plots at f_2 for pair of slots cut inside the CMSA for duroid substrate, (—) IE3D, (---) Proposed method

A. Results and Discussion

As observed from the dual frequencies and E plots (Figs. 5 to 7) for dual band CMSA with slots cut on the edges or inside the patch, a closer

prediction in resonant length (frequency) with $E \leq 5\%$ over entire slot length range is obtained. Also for U-slot cut CMSA (Figs. 8 to 10), a close match between the frequencies f_1 and f_2 , with $E \leq 5\%$ over entire slot length range is obtained. For duroid substrate also a close match between simulated and calculated frequencies is obtained. Similar results using RT-duroid substrate are obtained for U-slot cut CMSA. Thus the proposed formulations can be used in designing the antennas for any given substrate. For the suspended dual band CMSAs, the proposed equations can be used, by properly modifying the equation for the edge extension length.

III. CONCLUSIONS

The dual band CMSAs, realized by cutting a pair of rectangular slots or U-slot inside the patch, is analyzed for the modal variations over a wide frequency range for different slot dimensions. It has been observed that slots does not introduce any mode but reduces the higher order mode resonance frequency of CMSA and the dual band response is due to the modified TM_{11} and TM_{21} modes. By studying the current distributions at the dual frequencies, the resonant length formulation is proposed. This is obtained by modifying the equation for effective radius of the CMSA with respect to the slot length. The frequencies calculated using the proposed formulations agrees well with the simulated results with an error of less than 5% for different slot lengths and their positions inside the patch. The proposed formulations can be used to design the dual band CMSAs at the required frequencies, in various practical applications on any antenna substrate.

REFERENCES

- [1] G. Kumar and K. P. Ray, *Broadband Microstrip Antennas*, Artech House, USA, 2003
- [2] K. L. Wong, *Compact and Broadband Microstrip Antennas*, John Wiley & sons, Inc., New York, USA, 2002
- [3] A. E. Daniel and R. K. Shevgaonkar, "Slot-loaded rectangular microstrip antenna for tunable dual-band operation", *Microwave & Opti. Tech. Letters*, vol. 44, 5, 5th March 2005, pp. 441 – 444
- [4] J. H. Lu, 'Single feed dual frequency rectangular microstrip antenna with pair step slots', *Electronics Letters*, vol. 35, no. 5, 1999, pp. 354 – 355
- [5] A. A. Deshmukh and G. Kumar, "Even mode Multi-port Network Model for slotted dual band Rectangular Microstrip Antennas", *Microwave & Opti. Tech. Letters*, vol. 48, no. 4, 2006, pp. 798 – 804
- [6] K. P. Ray and D. D. Krishna, 'Compact dual band suspended semicircular microstrip antenna with half U-slot', *Microwave & Opti. Tech. Letters*, vol. 48, no. 10, 2006, pp. 2021 – 2024
- [7] K. R. Boyle and P. J. Massey, 'Nine band antenna system for mobile phones', *Electronics Letters*, vol. 42, no. 5, 2006, pp. 265 – 266
- [8] Amit A. Deshmukh and K. P. Ray, "Half U-slot loaded Multi-band Rectangular Microstrip Antennas", *International Journal of Microwave and Optical Technology*, vol. 2, no. 2, July 2007, pp. 216 – 221.
- [9] J. A. Ansari, Anurag Mishra, N. P. Yadav and P. Singh, "Dual-band Slot Loaded Circular Disk Patch Antenna for WLAN Application", *International Journal of Microwave and Optical Technology*, vol. 5, no. 3, May 2010, pp. 124 – 129.
- [10] Mohamed Nabil Srifi, Mourad Meloui and Mohamed Essaaidi, "Rectangular Slotted Patch Antenna for 5-6GHz Applications", *International Journal of Microwave and Optical Technology*, vol. 5, no. 2, March 2010, pp. 52 – 57.
- [11] J. B. Knorr and J. Saenz, "End effect in a shorted slot", *IEEE Trans. Microwave Theory & Techniques*, September 1973, pp. 579 – 580.
- [12] T. Huynh and K. F. Lee, "Single-Layer Single-Patch Wideband Microstrip Antenna," *Electronics Letters*, vol. 31, no. 16, August 1995, pp. 1310-1312.
- [13] R. Chair, K. F. Lee, C. L. Mak, K. M. Luk and A. A. Kishk, "Miniature Wideband Half U-Slot And Half E Patch Antennas," *IEEE Transactions On Antenna And Propagations*, vol. 52, no. 8, August 2005, pp. 2645-2652.
- [14] A. A. Deshmukh and G. Kumar, "Compact Broadband E-shaped Microstrip Antennas", *Electronics Letters*, vol. 41, no. 18, 2005, pp. 989 – 990
- [15] A. A. Deshmukh and G. Kumar, "Compact Broadband U-slot loaded Rectangular Microstrip Antennas", *Microwave & Opti. Tech. Letters*, vol. 46, no. 6, 2005, pp. 556 – 559
- [16] A. A. Deshmukh and G. Kumar, "Various slot loaded Broadband and Compact Circular Microstrip Antennas", *Microwave and Optical Technology Letters*, vol. 48, no. 3, Mar. 2006, pp. 435 – 439.
- [17] IE3D 12.1, Zeland Software, Fremont, USA, 2004.